

Fluorescent Nanosensor based on Molecularly Imprinted Polymers Coated on Graphene Quantum Dots for Fast Detection of Antibiotics

Tongchang Zhou; Arnab Halder; Yi Sun*

Department of Micro- and Nanotechnology, Technical University of Denmark, Ørstedes Plads, DK- 2800 Kgs, Lyngby, Denmark

*Corresponding Author: Sun.Yi@nanotech.dtu.dk.

Abstract:

In this work, we firstly explored a mild, clean, and highly efficient approach for the synthesis of graphene quantum dots (GQDs). GQDs with carboxyl groups or amino groups, were prepared from one-pot environmentally friendly method assisted by hydrogen peroxide, respectively. It was proved that carboxyl groups played an important role in the fluorescence quenching. Based on these findings, we developed a novel fluorescent nanosensor by combining molecularly imprinted polymers (MIPs) with carboxyl functionalized GQDs for the determination of tetracycline (TC) in aqueous samples. The nanocomposite was prepared using a sol-gel process. GQDs-MIPs showed strong fluorescent emission at 410 nm when excited at 360 nm, which was subsequently quenched in the presence of TC. Under optimum conditions, the fluorescence intensity of GQDs-MIPs decreased in response to the increase of TC concentration with good linearity range of $1.0\text{-}10^4 \mu\text{g L}^{-1}$. The limit of detection was determined to be $1 \mu\text{g L}^{-1}$. The fluorescence intensity of GQDs-MIPs was more strongly quenched by TC compared to the corresponding non-imprinted polymers, GQDs-NIPs. With the high sensitivity, the material was also successfully worked for the detection of TC in real spiked milk samples.

Key words: Graphene quantum dots, molecularly imprinted polymers, tetracycline, quenching

1. Introduction

Tetracycline (TC) is a kind of medicine commonly used for food-producing animals. Its residues in food products can cause various side effects to human bodies through the food chain. The overuse of these antibiotics is also believed to be responsible for the formation of antibiotic resistant strains of bacteria. The European Union has established the maximum residue limit of TC in milk ($100 \mu\text{g L}^{-1}$). MIPs have been prepared as biomimetic receptors for TC [1–4], classical analytical techniques such as UV, HPLC or other techniques have to be used to detect TC. High cost and complicated operation procedures limited

their application. Thus, a fast and suitable method is needed to monitor the residue of TC in food samples.

Molecular imprinting is a technique for the formation of molecularly imprinted polymers (MIPs) with tailor-made binding sites complementary to the template molecules in shape, size and functional groups [5–7]. In particular, fluorescent MIP-based sensors offer a convenient solution for analyte detection due to the high sensitivity and selectivity. They have many advantages, such as short analysis time, relatively simple to use, and requires small sample amounts. One simple way to prepare fluorescent MIPs is adding fluorescent monomers to MIP during synthesis [8,9]. However, fluorescence monomer normally involves complicated synthesis work. Quantum dots (QDs) are semiconductor nanocrystals that can provide narrow and tunable emission spectra [10]. Compared with organic dyes, QDs have attracted much more attention due to narrow symmetric emission bands, photochemical stability and good water dispersibility. These properties make them appropriate for the determination of analytes. Detection of analyte molecules by fabricating QDs has become a promising method in biological science. MIPs coated QDs sensors have been used for detection of amoxicillin [11], melamine [12], hemoglobin [13] and cytochrome c [14]. However, most work has used CdTe QDs, which displayed high cytotoxicity [15,16]. Therefore, environmentally friendly QDs are a better alternative and potentially safer to use in point-of-source applications.

Graphene quantum dots (GQDs) are a new class of carbon nanomaterial, which have lower toxicity and better biocompatibility than the traditional QDs [17,18]. GQDs have been directly used to detect cytochrome c [19]. By incorporating GQDs into MIP matrix, the nanocomposites will hold the specific physicochemical properties of the GQDs and the selective recognition properties of MIPs, which is interesting for application as nanosensor. GQDs have been widely prepared with graphene oxide (GO) as precursor via various methods. However, many methods for GQDs fabrication require strong acids, and long purification time. In addition, different fabrication and doping methods may result in different functional groups on the surface of GQDs, whereas the effects of functional groups on fluorescence quenching haven't yet been studied [20,21]. Furthermore, although MIPs-coated GQDs have been reported as nanosensor for detection of various compounds, directly detection of TC in food samples using GQDs embedded MIPs has not yet been demonstrated.

In our work, an efficient green synthetic strategy was applied to prepare GQDs with different functional groups in single step, respectively. We found that surface functional groups on GQDs played an important role in the fluorescence quenching. GQDs with carboxyl groups could be quenched by TC,

while no quenching was observed for GQDs with amino groups. MIPs coated on GQDs with carboxyl groups were synthesized using eco-friendly reaction solvent (mixture of water and ethanol) and used for determination of template TC with high sensitivity. The relative fluorescence intensity of GQDs-MIPs decreased linearly with increasing TC in the concentration range of $1 - 10^4 \mu\text{g L}^{-1}$ with a detection limit of $1 \mu\text{g L}^{-1}$. The GQDs-MIPs were also successfully applied to detect spiked TC in milk samples and gave recoveries from 85.3% to 103.3% with relative standard deviations of 3.7-7.2%. These results demonstrated that GQDs-MIPs could potentially be used as a simple and fast responding fluorescence probe for sensitive and selective determination of TC.

2. Materials and methods

2.1. Materials

All reagents were of analytical or HPLC grade and used as received. Aminopropyltriethoxysilane (APTES), Tetraethoxysilane (TEOS), Ammonium hydroxide solution (28%-30%), hydrogen peroxide (H_2O_2 , 30%), Gentamicin (GM) and amoxicillin (AM) and tetracycline (TC) were obtained from Sigma Aldrich. Nunclon 96-well flat-bottom black microwell plates were purchased from Thermo scientific, DK. 0.1% milk (Arla) was bought from a local supplier. The water used in the experiment was obtained from a Millipore (MilliQ) purification system.

2.2. Synthesis of two kinds of Graphene quantum dots (GQDs)

2.2.1. Synthesis of carboxylic acid functionalized Graphene quantum dots (GQDs-COOH)

To synthesize GQDs with carbonyl group, 40 mg of graphene oxide precursor was mixed with 30 mL of H_2O_2 (5%). Then the mixture was transferred into a 50 mL Teflon made autoclave chamber. The autoclave was put in an oven at 180°C for 2 h. After cooling down to room temperature, the resulting solution was filtered using $0.2 \mu\text{m}$ filter paper to remove unreacted graphene oxide, and the resulting filtrate was collected and stored at room temperature.

2.2.2. Synthesis of Amino functionalized Graphene quantum dots (GQDs-NH₂)

40 mg of graphene oxide precursor was mixed with 5 ml of H_2O_2 (30 %), 5 ml of NH_4OH (28-30 %) and 20 ml of water. The mixture was transferred into a 50 ml Teflon made autoclave chamber. The reaction mixture in the autoclave was kept in an oven at 180°C for 2h. After cooling down to room temperature, the resulting solution was filtered using a $0.2 \mu\text{m}$ filter paper, and the resulting filtrate was collected.

2.3. Preparation of GQDs-MIPs from sol-gel process

Briefly, 15 mL of GQDs (3 mg) solution and 10 mL of ethanol were added into a flask. Then 80 μL of APTES were added and stirred for 2 h under vigorous stirring to allow the APTES to self-assemble onto the GQDs. Template TC (10 mg) was then dissolved in ultrapure water (10 mL) and added to the above solution. After stirring for 15 min, 100 μL of ammonia hydroxide solution (25%) was added, then 100 μL of TEOS and 10 mL of ethanol were added drop by drop. The reaction mixture was stirred at room temperature for 24 h.

The final products GQDs-MIPs were collected by centrifugation, and were washed thoroughly with ethanol and MilliQ water. Non-imprinted particles (GQDs-NIPs) as a control were prepared similarly, except that the template was not added.

2.4. Characterization of GQDs-MIPs

TEM images were taken using a Tecnai T20 G2 (FEI, Oregon USA) transmission electron microscope. IR spectra was taken using a Spectrum 100 (PerkinElmer, MA, USA). X-ray photoelectron spectroscopy (XPS) analysis was carried out by Thermo Scientific™ K-Alpha™ XPS System with an Al K-Alpha (1486 eV) x-ray source.

2.5. Fluorescence measurement of GQDs-MIPs

TC with different concentrations (2 $\mu\text{g L}^{-1}$, 20 $\mu\text{g L}^{-1}$, 200 $\mu\text{g L}^{-1}$, 2000 $\mu\text{g L}^{-1}$ and $2 \times 10^4 \mu\text{g L}^{-1}$, 150 μL) and GQDs-MIPs solution (150 μL , 1 mg mL⁻¹) were sequentially injected into each well of a Nunclon 96-well flat-bottom black microplate. Then, the fluorescence spectra were measured with an excitation wavelength of 360 nm, using a Spark® multimode microplate reader (Tecan, Sweden). The fluorescent intensity at 410 nm was used for analyzing.

For detection of TC in milk, TC with the concentrations of 2 $\mu\text{g L}^{-1}$, 20 $\mu\text{g L}^{-1}$, 200 $\mu\text{g L}^{-1}$, 2000 $\mu\text{g L}^{-1}$ and $2 \times 10^4 \mu\text{g L}^{-1}$ were spiked into the milk (0.1%, Arla). The measurement was taken in the same manner as described above.

3. Results and discussion

3.1. Green synthesis of GQDs

It is of great significance and importance to explore a mild, clean, and highly efficient approach for the synthesis of GQDs. Generally, GQDs were synthesized by traditional methods such as electrochemical exfoliation [22], chemical oxidation [23] and microwave assisted methods [24]. Strong acids and

chemicals are often involved as oxidant in most approaches. Some amount of chemicals are left as residues in the resulted GQDs solution, which need repeated washing steps to get pure GQDs. Herein, we introduced a new green and rapid preparation approach for GQDs using a low amount of hydrogen peroxide as oxidant, as shown in Figure 1. As a degrading agent for graphene, H_2O_2 could cut down graphene into smaller sized graphene based QDs. The byproducts are only H_2O and CO_2 , and post purification step is not needed.

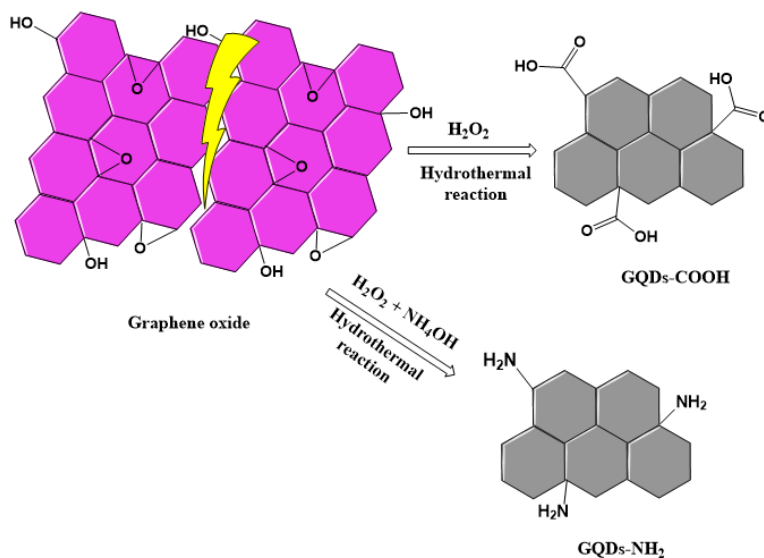


Figure 1. Illustration of the preparation of GQDs from graphene oxide.

3.2. Comparison of GQDs with different functional groups

As carbon-based materials, GQDs have excellent properties, such as high surface area and low toxicity. In addition, surface functional groups can effectively tune their properties, which can extend their application areas. In this work, we successfully prepared GQDs with two kinds of functional groups. Figure 2a shows FT-IR spectra of the functional groups on the GQDs. The sharp peak appearing at 1720 cm^{-1} and 1226 cm^{-1} belonged to the C=O stretching and C-O stretching of carboxylic acid, respectively. In the meantime, a band appeared at 1576 cm^{-1} was assigned to C-N stretching while the band appearing at 1291 cm^{-1} was assigned to the mixed vibration of C-N stretching and N-H bending. The detailed surface chemical bonding nature of GQDs-COOH and GQDs-NH₂ were evaluated using XPS. As shown in Figure 2b, both of GQDs-COOH and GQDs-NH₂ showed C 1s and O 1s peaks at around 286 eV and 532 eV. However, only a new peak was observed for GQDs-NH₂ at around 400 eV, which was due to the presence of nitrogen. The C 1s spectra of GQDs-COOH was further deconvoluted into two peaks with

binding energies at 284.9 and 288.7 eV, which correspond to sp² and sp³ hybridized carbon (C-C/C=C) and O-C=O components respectively (Figure 2c).

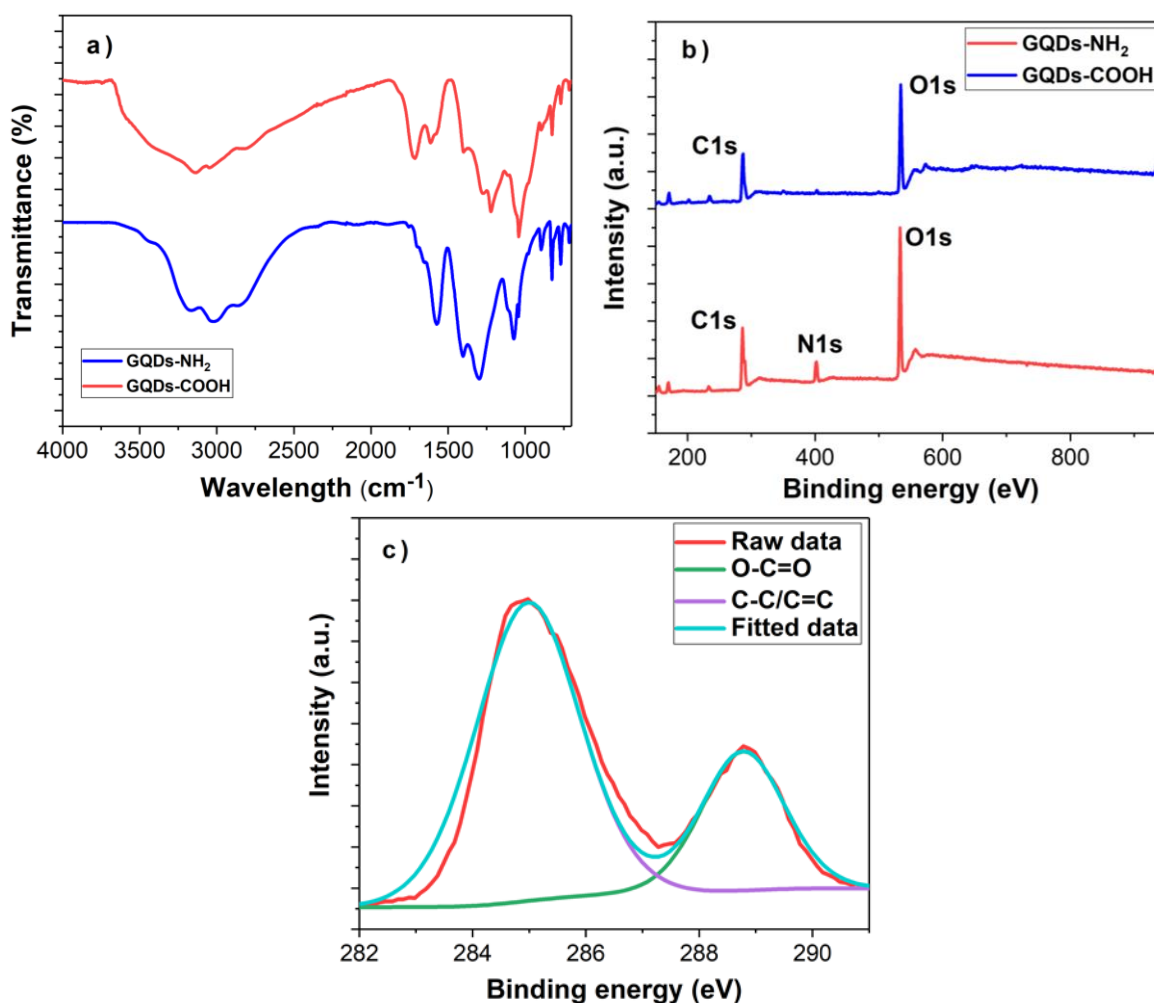


Figure 2. (a) FTIR of two types of GQDs. (b) XPS survey spectra for GQDs-COOH and GQDs-NH₂. (c) The high resolution deconvoluted C 1s spectra for GQDs-COOH.

To compare these GQDs with different functional groups, we tested the fluorescence emission spectra of GQDs with the addition of TC solutions. Quenching of GQDs-COOH was observed at the concentration at and above $10^4 \mu\text{g L}^{-1}$, as shown in Figure 3a. In comparison, the fluorescence of GQDs-NH₂ could not be quenched in the presence of TC. Quenching requires molecular contact and energy transfer between the fluorophore and quencher. Here GQDs-COOH was negatively charged while GQDs-NH₂ was positively charged. In the meantime, ammonium groups of TC was positively charged. Therefore, electrostatic interaction occurred between GQDs-COOH and the template TC, which resulted in the apparent nonradiative annihilation, as reported by Chao [25]. In addition, this was further proved by the

zeta potential results of GQDs-COOH, which was found to be -27.6 mV in water. Therefore, MIPs based on GQDs-COOH were applied for further experiments.

The study the quenching mechanism, the absorption spectra of GQDs-COOH in the presence and absence of TC were measured as illustrated in Figure 3b. It was observed that the absorbance of GQDs changed with the addition of TC, indicating the interaction between GQDs and TC induced static quenching, as static quenching affects the absorption spectrum of quenching molecule.

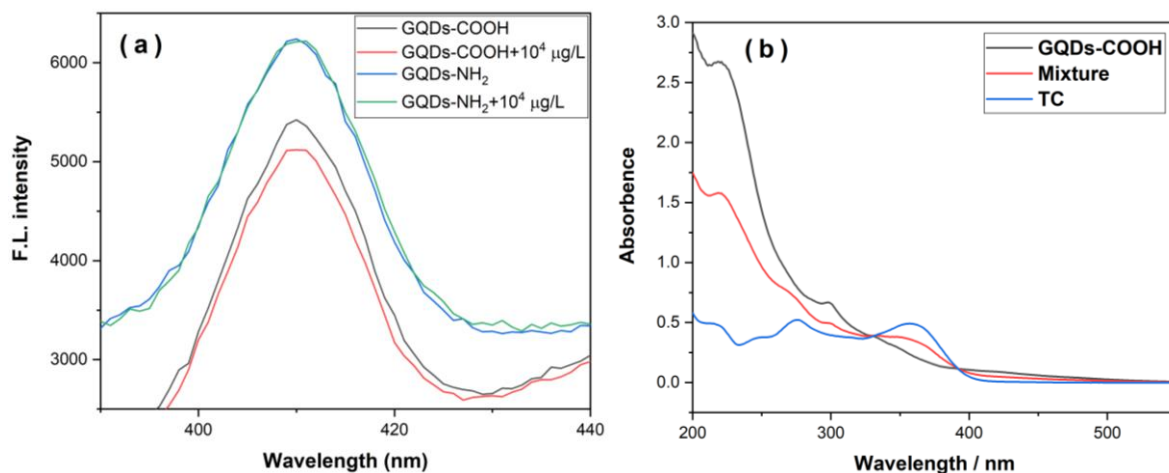


Figure 3. (a) Fluorescence emission spectra of GQDs with different functional groups with addition of TC in water. (b) UV spectrum of GQDs-COOH, TC and mixture.

3.3. TEM of GQDs-MIP and GQDs

MIP and reference NIP were successfully synthesized by sol-gel process. The morphology and size distribution of GQDs, GQDs-MIPs and GQDs-NIPs were investigated by TEM, as illustrated in Figure 4. The GQDs had a good size distribution around 5 nm while both the GQDs-MIPs and GQDs-NIPs exhibited a size distribution with diameters in the range of 200-300 nm. After the coating of MIPs on GQDs, it is clear that the particles diameters increased significantly.

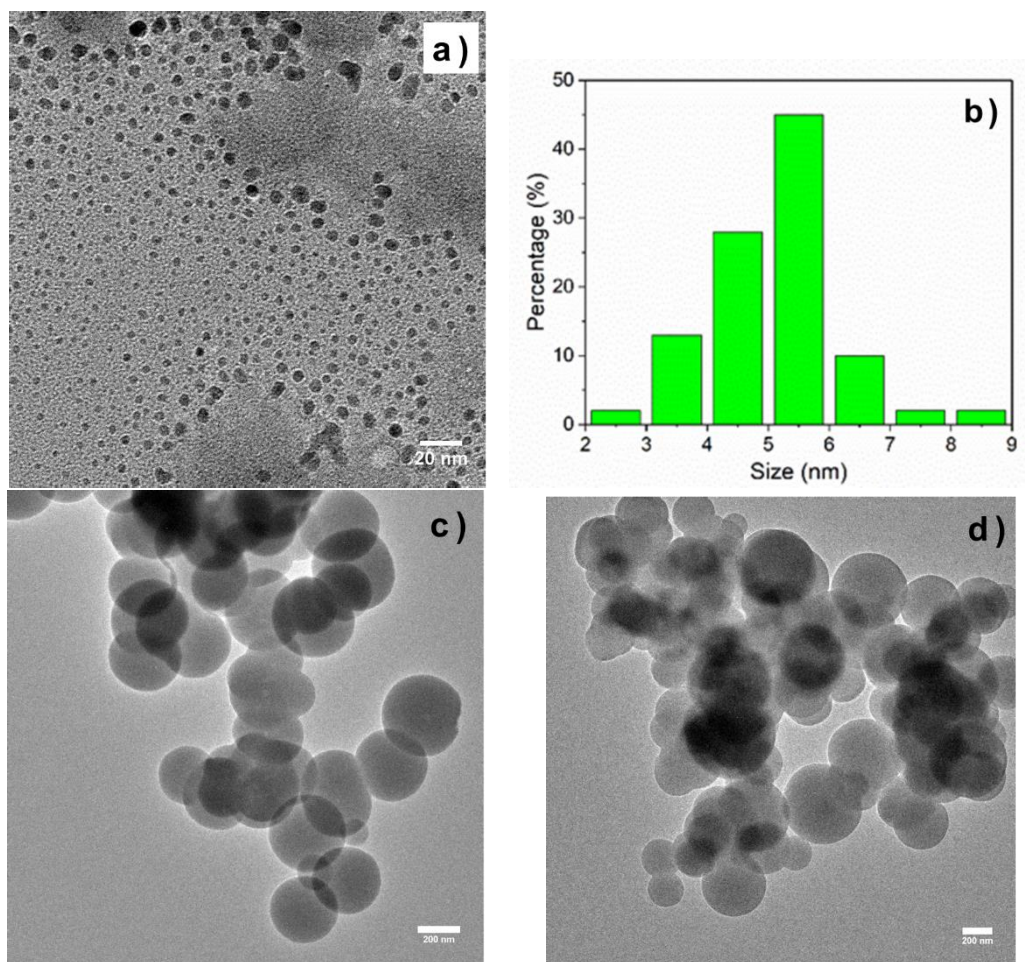


Figure 4. TEM images of GQDs (a), GQDs-MIPs (c), and GQDs-NIPs (d). The hydrodynamic size distribution of GQDs (b).

3.4. Determination of TC using GQDs-MIPs

To study the recognition ability of GQDs-MIPs, the fluorescence intensity change of GQDs-MIPs and GQDs-NIPs were investigated at different concentration of TC, which are shown in Figure 5a and Figure 5b. Although both GQDs-MIPs and NIPs showed fluorescence quenching response to TC, the intensity of GQDs-MIPs decreased more significantly in response to the increase of TC concentration compared with GQDs-NIPs. It is clear that specific cavities of MIPs resulted in the higher quenching efficiency of GQDs-MIPs. The results showed that the GQDs-MIPs exhibited a linear quenching for the TC detection in the range of $1.0\text{-}10^4 \mu\text{g L}^{-1}$, and the limit of detection for TC was determined to be $1 \mu\text{g L}^{-1}$ under optimal conditions (Figure 5c). Normally, a certain incubation time is needed for sufficient interactions between analytes and GQDs-MIPs. It worth noting that here all the tests were measured immediately after TC solution was mixed with GQDs-MIPs, suggesting that the response time of the developed sensor was

very short and the quenching occurred rapidly. This is very helpful for fast detection of TC in real samples.

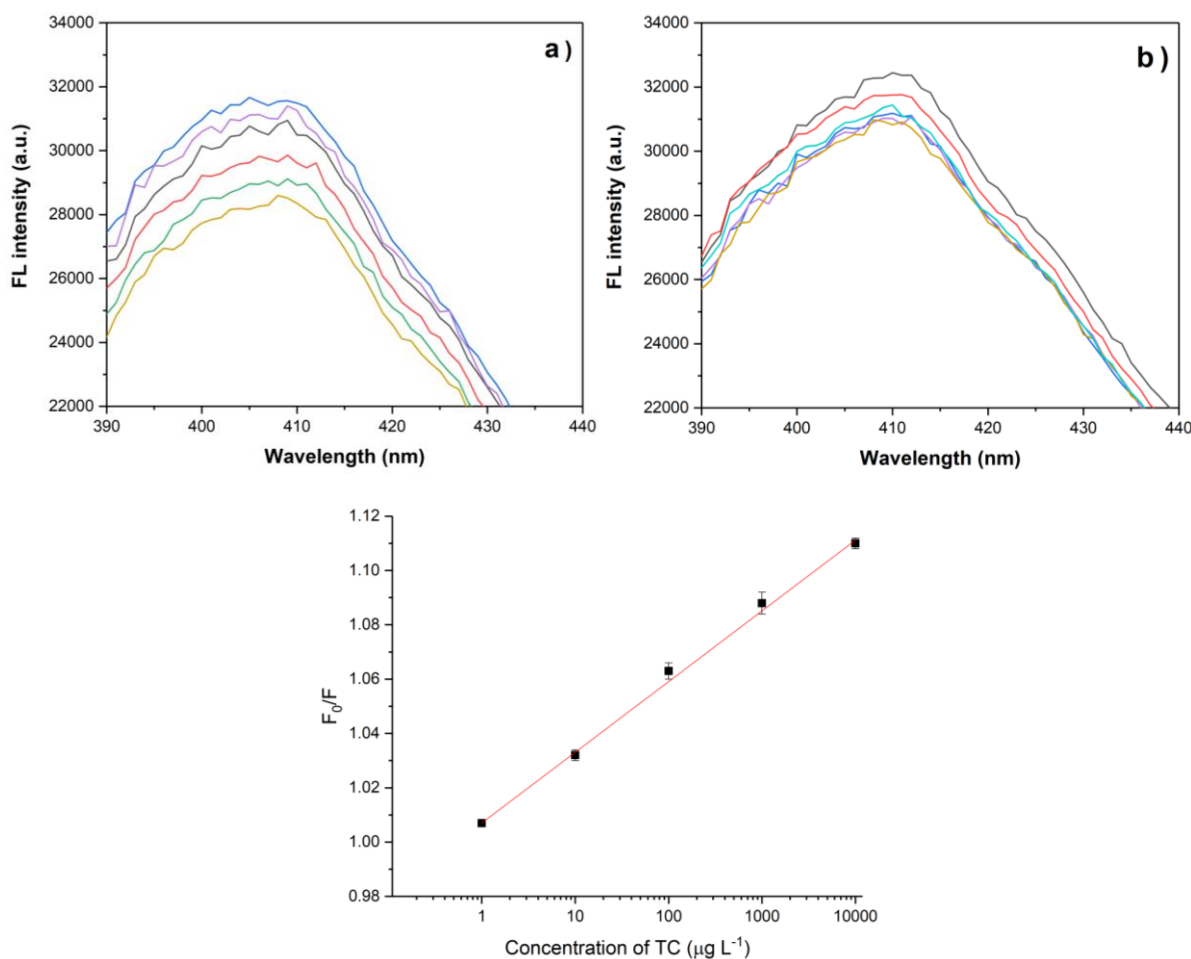


Figure 5. Fluorescence emission spectra of GQDs-MIPs (a) and GQDs-NIPs (b) with addition of various amount of TC in water. F_0 and F represent the fluorescent intensities before and after addition of TC solution, respectively.

3.5. Selectivity of GQDs-MIPs

The selectivity of the GQDs-MIPs was further investigated by fluorescence quenching response to analyte with similar structure to TC. One interference compound was doxycycline (DOX), a synthetic antibiotic derived from TC. The chemical differences between them are in the substituents of some carbon atoms, as shown clearly in Figure 6. Because of the efficiency of molecularly imprinting, we found that the template TC bound more strongly to the imprinted sites than DOX, and more significantly change in the fluorescence intensity of GQDs-MIPs were observed. Due to big structure difference with TC, the quenching of GQDs-MIPs by Gentamicin (GM) and amoxicillin (AM) were quite small. The above results revealed that GQDs-MIPs exhibited a selective recognition and excellent fluorescence quenching

response toward TC. As the molecular size and shape are very similar between TC and DOX, the position of the functional groups is the major dominating factors for a specific fluorescence quenching response.

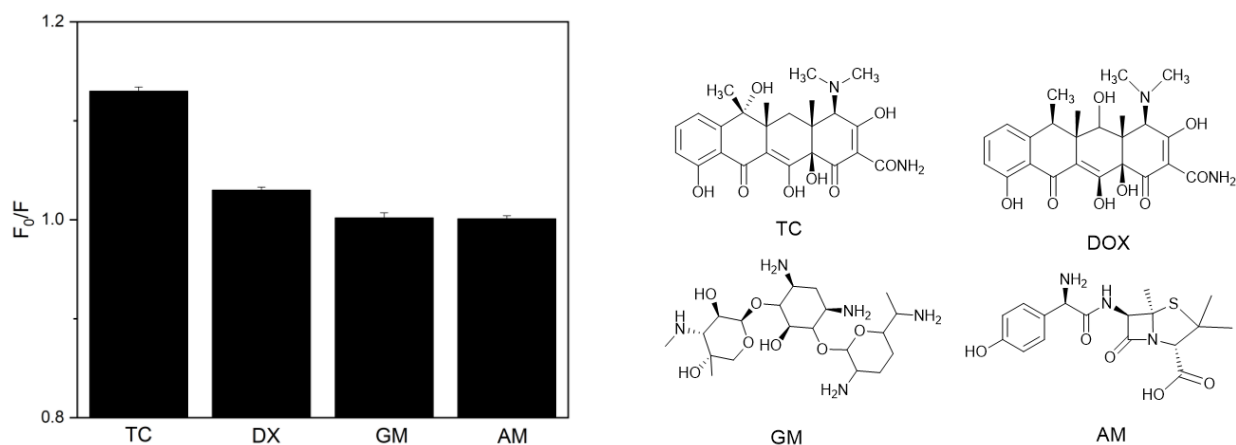


Figure 6. Selective adsorption of TC, DOX, GM and AM by GQDs-MIPs in water. The concentration of all compounds was $10^4 \mu\text{g L}^{-1}$.

3.6. Real sample analysis

To further demonstrate the selectivity and sensitivity of GQDs-MIPs, detection and quantification of TC in real milk samples were conducted. According to the results shown in Table 1, the spiked recoveries of TC ranged from 85.3% to 103.3%, which indicated good accuracy and low detection of limit. The results suggested that the combination of GQDs and MIPs was an effective method for analyzing antibiotic residues in complex food samples.

Table 1. Results of the analysis of the milk samples

Samples	Spiked Amount ($\mu\text{g L}^{-1}$)	Measured Amount ($\mu\text{g L}^{-1}$)	Recovery (%)
1	1	0.98 ± 0.049	98 ± 4.9
2	10	9.22 ± 0.57	92.2 ± 5.7
3	100	103.3 ± 3.7	103.3 ± 3.7
4	10^3	$(9.74 \pm 0.72) \times 10^2$	97.4 ± 7.2
5	10^4	$(8.53 \pm 0.61) \times 10^3$	85.3 ± 6.1

4. Conclusion

Nowadays, rapid and efficient detection methods for the trace amounts of antibiotics food samples are in urgent need for food security screening. In this work, GQDs were fabricated via a simple and green synthesis approach, and the effect of functional groups on fluorescence quenching was investigated. A GQDs-MIPs based fluorescence nanosensor was then successful prepared by a simple sol-gel method. The results showed fast detection and selectivity. Compared with natural bioassay, these materials have

higher stability and lower cost. The work suggested that QGDs-MIPs could be used efficiently to screen and analyze TC in food samples.

Conflict of interest

The authors declare no competing financial interest.

Acknowledgement

This work was financially supported by the Villum Fonden, Denmark, Project NO. 13153.

Reference

1. Chen, L.; Liu, J.; Zeng, Q.; Wang, H.; Yu, A.; Zhang, H.; Ding, L. Preparation of magnetic molecularly imprinted polymer for the separation of tetracycline antibiotics from egg and tissue samples. *J. Chromatogr. A* **2009**, *1216*, 3710–3719.
2. Jing, T.; Gao, X. D.; Wang, P.; Wang, Y.; Lin, Y. F.; Hu, X. Z.; Hao, Q. L.; Zhou, Y. K.; Mei, S. R. Determination of trace tetracycline antibiotics in foodstuffs by liquid chromatography-tandem mass spectrometry coupled with selective molecular-imprinted solid-phase extraction. *Anal. Bioanal. Chem.* **2009**, *393*, 2009–2018.
3. Lv, Y. K.; Zhao, C. X.; Li, P.; He, Y. D.; Yang, Z. R.; Sun, H. W. Preparation of doxycycline-imprinted magnetic microspheres by inverse-emulsion suspension polymerization for magnetic dispersion extraction of tetracyclines from milk samples. *J. Sep. Sci.* **2013**, *36*, 2656–2663.
4. Shen, X.; Svensson Bonde, J.; Kamra, T.; Bülow, L.; Leo, J. C.; Linke, D.; Ye, L. Bacterial imprinting at pickering emulsion interfaces. *Angew. Chemie - Int. Ed.* **2014**, *53*, 10687–10690.
5. Bedwell, T. S.; Whitcombe, M. J. Analytical applications of MIPs in diagnostic assays: future perspectives. *Anal. Bioanal. Chem.* **2016**, *408*, 1735–1751.
6. Liu, L.; Yang, K.; Zhang, L.; Zhang, Y. Protein-imprinted material for the treatment of antibiotic-resistant bacteria. *Sci. Bull.* **2016**, *61*, 1890–1891.
7. Chen, L.; Wang, X.; Lu, W.; Wu, X.; Li, J. Molecular imprinting: Perspectives and applications. *Chem. Soc. Rev.* **2016**, *45*, 2137–2211.
8. Wan, W.; Biyikal, M.; Wagner, R.; Sellergren, B.; Rurack, K. Fluorescent sensory microparticles that “light-up” consisting of a silica core and a molecularly imprinted polymer (MIP) shell. *Angew. Chemie - Int. Ed.* **2013**, *52*, 7023–7027.
9. Ashley, J.; Feng, X.; Sun, Y. A multifunctional molecularly imprinted polymer-based biosensor for direct detection of doxycycline in food samples. *Talanta* **2018**, *182*, 49–54.
10. Yang, Y.; Yi, C.; Luo, J.; Liu, R.; Liu, J.; Jiang, J.; Liu, X. Glucose sensors based on electrodeposition of molecularly imprinted polymeric micelles: A novel strategy for MIP sensors. *Biosens. Bioelectron.* **2011**, *26*, 2607–2612.
11. Chullasat, K.; Nurerk, P.; Kanatharana, P.; Davis, F.; Bunkoed, O. A facile optosensing protocol based on molecularly imprinted polymer coated on CdTe quantum dots for highly sensitive and selective amoxicillin detection. *Sensors Actuators, B Chem.* **2018**, *254*, 255–263.

12. Xu, S.; Lu, H. One-pot synthesis of mesoporous structured ratiometric fluorescence molecularly imprinted sensor for highly sensitive detection of melamine from milk samples. *Biosens. Bioelectron.* **2015**, *73*, 160–166.
13. Zhang, W.; He, X. W.; Chen, Y.; Li, W. Y.; Zhang, Y. K. Composite of CdTe quantum dots and molecularly imprinted polymer as a sensing material for cytochrome c. *Biosens. Bioelectron.* **2011**, *26*, 2553–2558.
14. Li, D.-Y.; He, X.-W.; Chen, Y.; Li, W.-Y.; Zhang, Y.-K. Novel Hybrid Structure Silica/CdTe/Molecularly Imprinted Polymer: Synthesis, Specific Recognition, and Quantitative Fluorescence Detection of Bovine Hemoglobin. *ACS Appl. Mater. Interfaces* **2013**, *5*, 12609–12616.
15. Fang, T. T.; Li, X.; Wang, Q. S.; Zhang, Z. J.; Liu, P.; Zhang, C. C. Toxicity evaluation of CdTe quantum dots with different size on *Escherichia coli*. *Toxicol. Vitr.* **2012**, *26*, 1233–1239.
16. Yang, Q.; Li, J.; Wang, X.; Peng, H.; Xiong, H.; Chen, L. Strategies of molecular imprinting-based fluorescence sensors for chemical and biological analysis. *Biosens. Bioelectron.* **2018**, *112*, 54–71.
17. Gravagnuolo, A. M.; Morales-Narvez, E.; Longobardi, S.; Da Silva, E. T.; Giardina, P.; Merkoçi, A. In situ production of biofunctionalized few-layer defect-free microsheets of graphene. *Adv. Funct. Mater.* **2015**, *25*, 2771–2779.
18. Mehrzad-Samarin, M.; Faridbod, F.; Dezfouli, A. S.; Ganjali, M. R. A novel metronidazole fluorescent nanosensor based on graphene quantum dots embedded silica molecularly imprinted polymer. *Biosens. Bioelectron.* **2017**, *92*, 618–623.
19. Cao, L.; Li, X.; Qin, L.; Kang, S.-Z.; Li, G. Graphene quantum dots supported by graphene oxide as a sensitive fluorescence nanosensor for cytochrome c detection and intracellular imaging. *J. Mater. Chem. B* **2017**, *5*, 6300–6306.
20. Zhou, X.; Wang, A.; Yu, C.; Wu, S.; Shen, J. Facile Synthesis of Molecularly Imprinted Graphene Quantum Dots for the Determination of Dopamine with Affinity-Adjustable. *ACS Appl. Mater. Interfaces* **2015**, *7*, 11741–11747.
21. Amjadi, M.; Jalili, R. Molecularly imprinted polymer-capped nitrogen-doped graphene quantum dots as a novel chemiluminescence sensor for selective and sensitive determination of doxorubicin. *RSC Adv.* **2016**, *6*, 86736–86743.
22. Li, Y.; Hu, Y.; Zhao, Y.; Shi, G.; Deng, L.; Hou, Y.; Qu, L. An electrochemical avenue to green-luminescent graphene quantum dots as potential electron-acceptors for photovoltaics. *Adv. Mater.* **2011**, *23*, 776–780.
23. Liu, R.; Wu, D.; Feng, X.; Müllen, K. Bottom-up fabrication of photoluminescent graphene quantum dots with uniform morphology. *J. Am. Chem. Soc.* **2011**, *133*, 15221–15223.
24. Hou, J.; Li, H.; Wang, L.; Zhang, P.; Zhou, T.; Ding, H.; Ding, L. Rapid microwave-assisted synthesis of molecularly imprinted polymers on carbon quantum dots for fluorescent sensing of tetracycline in milk. *Talanta* **2016**, *146*, 34–40.
25. Chao, M. R.; Hu, C. W.; Chen, J. L. Comparative syntheses of tetracycline-imprinted polymeric silicate and acrylate on CdTe quantum dots as fluorescent sensors. *Biosens. Bioelectron.* **2014**, *61*, 471–477.